ELSEVIER

# A new candidate cathode material as (Co/Mg)-coated Ni powder for molten carbonate fuel cell[☆]

Eunjoo Park[a,*], Mingzi Hong[b], Hyunsuk Lee[a], Minhyuk Kim[a], Keon Kim[a,**]

[a] *Division of Chemistry and Molecular Engineering, Korea University, South Korea*
[b] *Jilin Institute of Chemical Technology, Julin 132022, China*

## Abstract

Co/Mg solid solution coated Ni powder, where Mg-doped LiCoO$_2$ is coated on NiO in molten carbonate, has been used as a new cathode material to reduce the solubility of NiO and to maintain the advantages of NiO cathode. The (Co/Mg)-coated NiO cathode was prepared by a coating Co/Mg solid solution on the surface of the Ni powder using a PVA assisted sol–gel method. The phase changes of the (Co/Mg)-coated Ni powder after immersed into Li/K eutectic carbonate mixtures at 550 °C ∼ 850 °C for 48 h was performed by XRD and Raman. SEM was used to study the particle morphologies. Co/Mg solid solution was coated on the surface of the Ni powder and Li(NiCoMg)O$_2$ is formed on NiO in molten carbonate. It is expected that the Li(NiCoMg)O$_2$ phase will reduce the solubility of NiO cathode in molten carbonate.
© 2004 Elsevier B.V. All rights reserved.

*Keywords:* Solubility; MCFC; (Co/Mg)-coated NiO cathode; Sol–gel method

## 1. Introduction

Nickel oxide (NiO) is commonly used as the cathode for the molten carbonate fuel cell (MCFC) for its stability in carbonate melt and an oxygen atmosphere and because of its high electrical conductivity. But the dissolution of the state of the art cathode material NiO into the electrolyte is one of the major technical obstacles to the commercialization of the MCFC [1–3]. NiO is known for dissolving into molten carbonate by an acidic dissolution mechanism [4]. This dissolution leads to the formation of Ni$^{2+}$, which diffuses, from the cathode toward the anode under a concentration gradient. The dissolved Ni$^{2+}$ precipitates in the matrix, where it encounters dissolved H$_2$ proceeding from the anode side. Continuous deposition of metallic nickel across the cell forms bridged grains and eventually short-circuiting of the cell [5,6]. Lots of studies

have been carried out to solve this problem [7–12]. One was to adjust the composition of the carbonates to retard dissolution of nickel oxide and the other was to find an alternative material to replace nickel oxide. Currently, LiCoO$_2$ seems to be one of the best candidate materials due to its higher stability and lower solubility than NiO in molten carbonate. Also, it has a lower but still acceptable electrical conductivity for the MCFC cathode [8]. However, application of LiCoO$_2$ as a new cathode has problems for the scaled-up electrode area because LiCoO$_2$ sheet is too brittle, and because LiCoO$_2$ has a relatively high manufacturing cost [9,13–16]. Therefore, many investigators have attempted to obtain an alternative cathode such as a Co-coated Ni cathode. This cathode has lower solubility and higher electrochemical performance than that of the NiO cathode [17–19]. However, further studies are necessary in order to reduce solubility and to improve the electrochemical performance of the cathode for the MCFC.

The conductivity of LiCoO$_2$ at room temperature can be increased by over two orders of magnitude by partial substitution of Co$^{3+}$ with Mg$^{2+}$ [20,21]. MgO is known to make a solid solution with Co$_3$O$_4$ at any ratio [22]. In this study, a Co/Mg solid solution coated Ni powder, where Mg doped
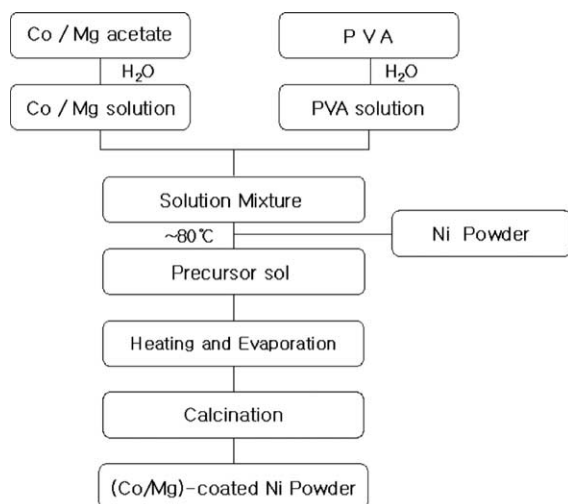
Fig. 1. Experimental procedure for preparation of (Co/Mg)-coated Ni powder using PVA assisted sol–gel method.

LiCoO$_2$ is coated on to NiO in molten carbonate, has been synthesized as a new cathode material to reduce the solubility of the cathode and to maintain the advantages of the NiO cathode.

## 2. Experimental

### 2.1. Preparation of (Co/Mg)-coated Ni powder

The (Co/Mg)-coated Ni powder was prepared from a Co/Mg solid solution by a PVA assisted sol–gel method. This procedure is illustrated in Fig. 1. Stoichiometrically, Cobalt(II) acetate tetrahydrate [(CH$_3$COOCo)$_2$·4H$_2$O, >98%, Aldrich] and magnesium acetate tetrahydrate [(CH$_3$COOMg)$_2$·4H$_2$O, >99%, Aldrich] were dissolved in distilled water. Another solution as a chelating agent was prepared by dissolving polyvinyl alcohol (PVA, degree of polymerization 1500, Junsei) in distilled water with mechanical stirring. The molar ratio of PVA versus metal ions in the solution was 6:1. While the PVA solution was constantly stirred, the metal acetate solution was well mixed with the polymer solution. The Ni powder was added to the mixed solution. The resultant solution was heated at 70–80 °C and constantly stirred until the precursor gel was produced. The precursor gel was calcined at 500 °C for 3 h to obtain the (Co/Mg)-coated Ni powders.

### 2.2. Lithiation of the (Co/Mg)-coated Ni powder

In order to investigate the phase change of the (Co/Mg)-coated Ni powder with different (Co/Mg) mole fractions under the actual MCFC operation conditions, the lithiation treatment was performed at various temperatures (550, 650, 750 and 850 °C) in (Li$_{0.62}$K$_{0.38}$)$_2$CO$_3$ under a CO$_2$:O$_2$ (67:33%) atmosphere for 48 h. The carbonate on the lithiated powder was cleaned with 1 M CH$_3$COOH, and then the powder was washed with distilled water and dried in an oven. After drying, the composition and the surface morphology of the powders were analyzed with XRD, Raman spectrometry and SEM.

### 2.3. Preparation of the (Co/Mg)-coated NiO cathode

The (Co/Mg)-coated Ni cathode was made by the usual tape-casting method. Binder (0.3 g, MC1500, Hanawa Co., Japan), plasticizer (1.38 g, glycerol, Junsei Co., Japan), and deformer (0.3 g, SN1540, San Nopco Ltd., Korea) were added into the solvent (H$_2$O) for ball milling for 24 h. Then (Co/Mg)-coated Ni powder (30 g) and dispersant (0.3 g, Cerasperse 5468, San Nopco Ltd., Korea) were added and ball-milled for 4 h. After ball milling, the slurry was completely degassed using a ROTOVAP evaporator. The slurry was tape-cast with a double doctor blade assembly to get a cathode green sheet. The (Co/Mg)-coated Ni sheet was dried slowly at room temperature for 24 h. After drying, it was heat treated (with a rate of 3 °C min$^{-1}$) under a reducing atmosphere (H$_2$) at 1000 °C for 2 h.

### 2.4. Solubility test

The solubility of the (Co/Mg)-coated Ni cathode was measured in a (Li$_{0.62}$K$_{0.38}$)$_2$CO$_3$ eutectic melt. The same experimental apparatus for the Co-coated Ni cathode solubility measurement was used [17]. 1.5 g of (Co/Mg)-coated Ni cathode was immersed into 100 g (Li$_{0.62}$K$_{0.38}$)$_2$CO$_3$. The inlet gas was a CO$_2$:O$_2$ (67:33) gas mixture, which was blown in at 650 °C. Equilibrium solubility was determined by removing a ∼0.3 g aliquot of molten carbonate from the melts at the appointed time using an alumina pipette. Each liquid carbonate sample was transferred to a clean alumina crucible, where it solidified. Then the sample was dissolved in 1 M HNO$_3$ to analyze the concentration of Ni dissolved into the carbonate melt by inductively coupled plasma atomic emission spectroscopy (ICP–MS).

## 3. Results and discussion

### 3.1. The (Co/Mg)-coated Ni powders

TGA and DSC results of the gel precursors are shown in Fig. 2. The weight loss of the gel precursors terminated near 500 °C in three discrete steps. The first weight loss step occurred between 150 and 200 °C due to water evaporation and showed an endothermic reaction curve. The second weight loss step between 350 and 400 °C was attributed to the removal of the acetate. The last weight loss step showed an exothermic reaction curve between 400 and 500 °C because of the combustion of PVA and organic residues. When the temperature rose beyond 500 °C, a slow weight gain appeared due to the oxidation of the metal surface. According to the
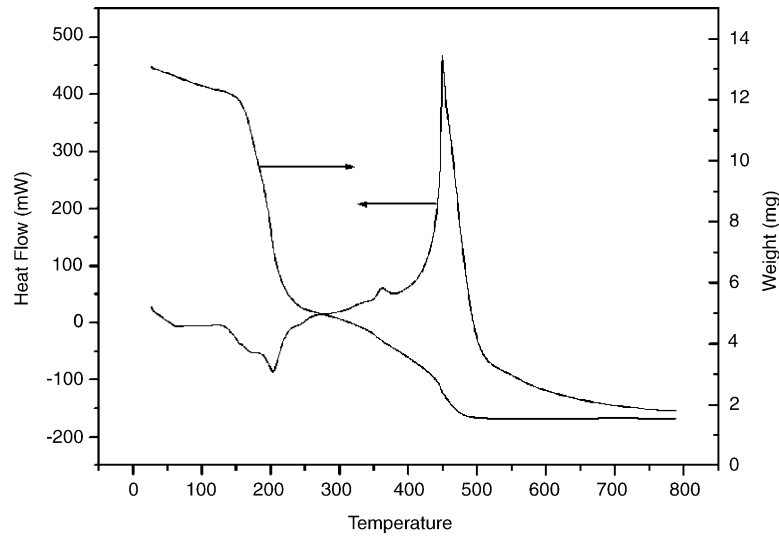
Fig. 2. TGA–DSC curves for the (Co/Mg)/Ni precursor.

TGA and DSC curves, the calcinations temperature of the gel precursor should be 500 °C.

Fig. 3 shows the XRD patterns of the (Co/Mg)-coated Ni powder obtained after calcination treatment of the gel precursor at various temperatures in air for 3 h. As the temperature increases, the intensities of the XRD peaks for Ni decrease accordingly, and those of NiO increase. Also, the XRD patterns showed major peaks of $Co_3O_4$ at 19.016, 31.298, 36.883, 44.848, 59.411 and 65.297° ($2\theta$) when the (Co/Mg)-coated Ni powder precursor was calcined above 400 °C. As the tem-
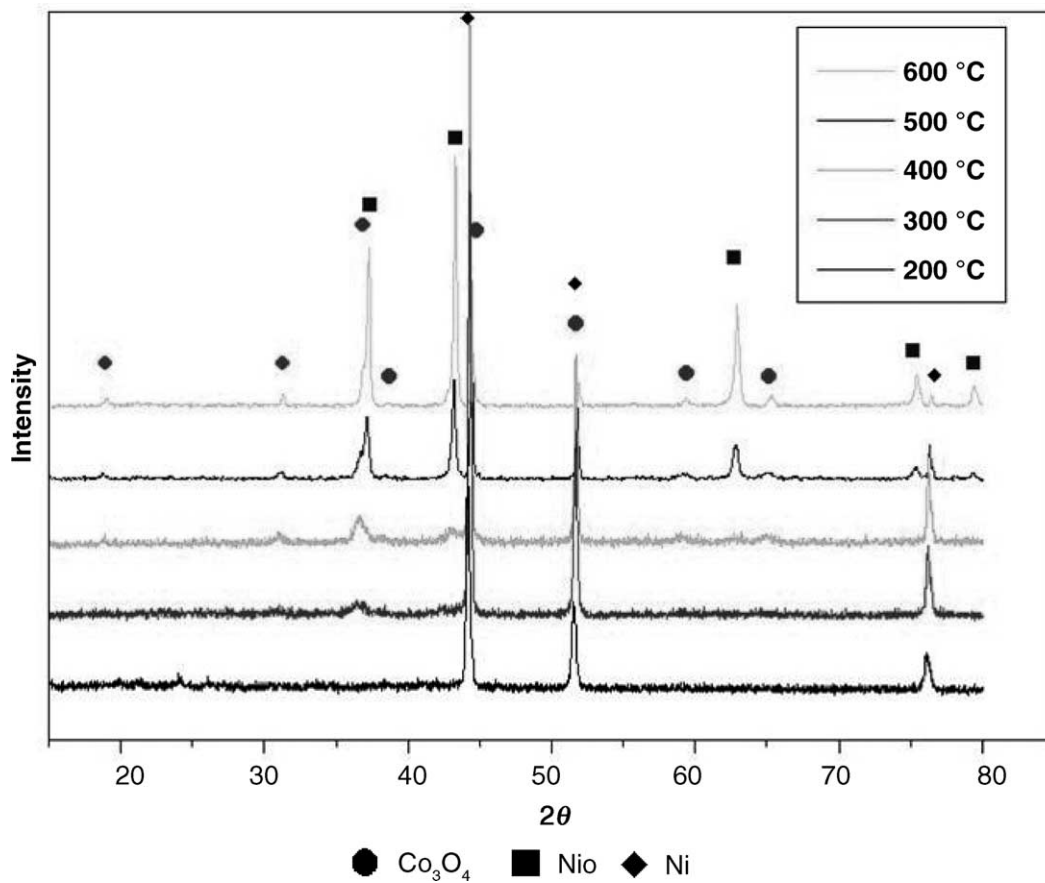


Fig. 3. XRD patterns of the (Co/Mg)-coated Ni powder after heat treatment at various temperatures.
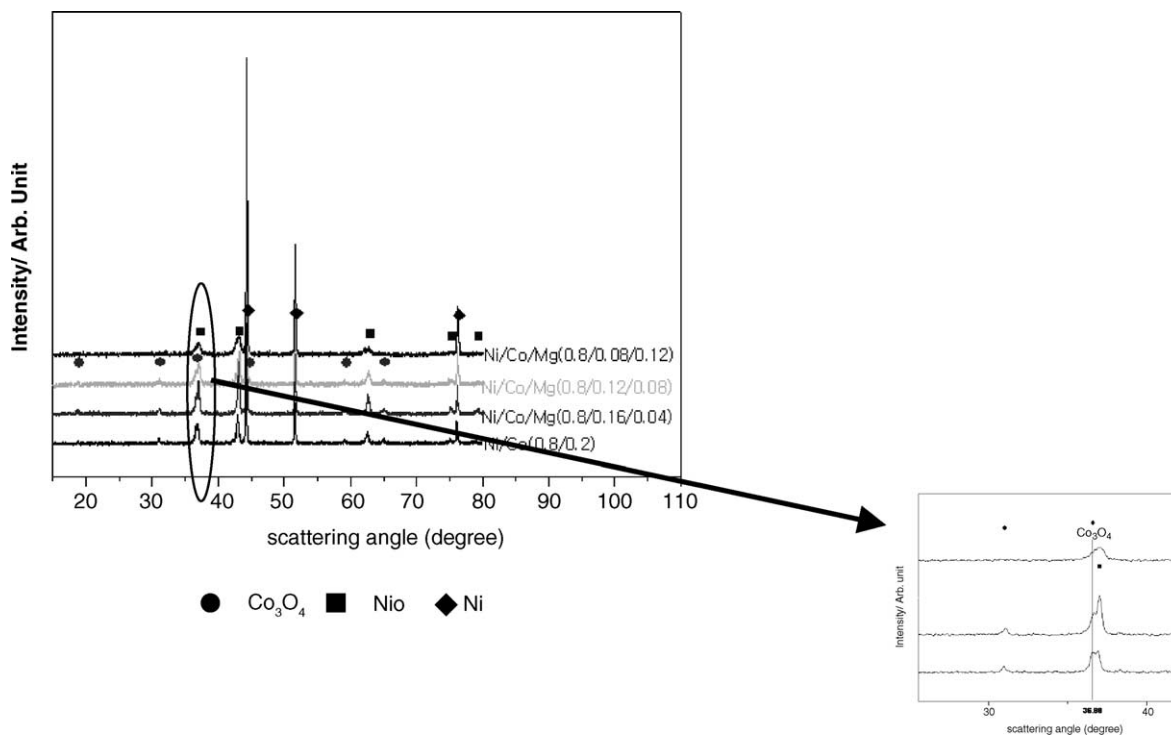
Fig. 4. XRD patterns of (Co/Mg)-coated Ni powder with different (Co/Mg) mole fractions after calcination at 500 °C.

perature increases, the peaks of $Co_3O_4$ were shifted to higher angle because of the formation of a Co/Mg solid solution on the surface of the Ni powers.

Fig. 4 shows XRD patterns of the (Co/Mg)-coated Ni powders with a different (Co/Mg) mole fraction after calcination at 500 °C. As the amount of Mg increases, the major peaks of $Co_3O_4$ at 36.88° were shifted to a higher angle. Fig. 5 shows SEM images of the (Co/Mg)-coated Ni powders after calcinations at 500 °C. From these SEM images, we can see that the surface of the Ni powder is covered with small particles. Therefore, we may guess that the small particles coated on the surface of the Ni powders are the Co/Mg solid solution.

### 3.2. Lithiated (Co/Mg)-coated Ni powders

In order to investigate the phase change of the (Co/Mg)-coated Ni powder in the molten carbonate, lithiation treatment was performed at various temperatures (550–850 °C) in $(Li_{0.62}K_{0.38})_2CO_3$ under air atmosphere for 48 h. The XRD patterns of the lithiated (Co/Mg)-coated Ni powders are shown in Fig. 6. Based on the XRD patterns, the lithiated (Co/Mg)-coated Ni powders show two different structure types. The XRD peaks of NiO appear at 37.312, 43.334, 62.974, 75.516 and 79.479°, and those of $LiCoO_2$ at 18.947, 37.425, 45.281, 59.640 and 65.494° ($2\theta$) after the (Co/Mg)-



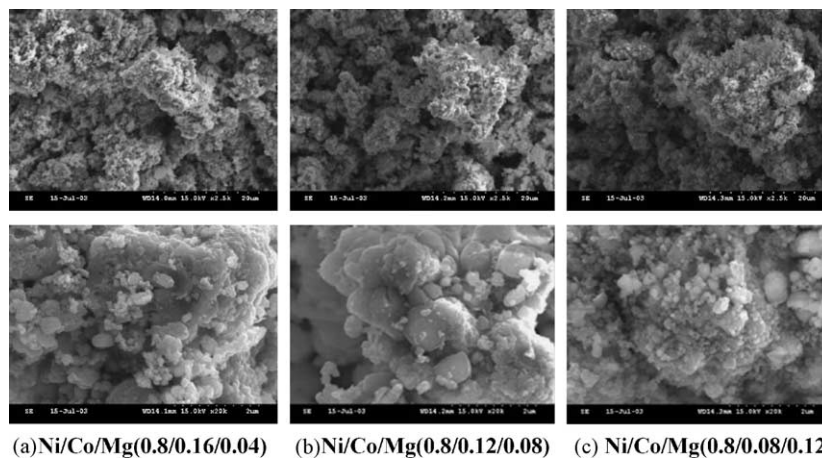(a) Ni/Co/Mg(0.8/0.16/0.04)　　(b) Ni/Co/Mg(0.8/0.12/0.08)　　(c) Ni/Co/Mg(0.8/0.08/0.12)

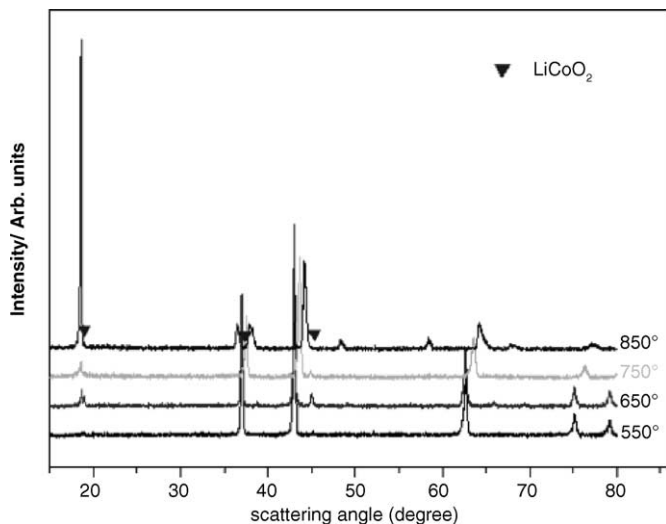Fig. 5. SEM images of the (Co/Mg)-coated Ni powders with different (Co/Mg) mole fractions after calcination at 500 °C.

Fig. 6. XRD patterns of the (Co/Mg)/Ni after immersion in Li/K carbonate at various temperatures for 48 h.

the $LiCoO_2$ were shifted to a higher angle direction due to Mg diffused into $LiCoO_2$ to form $Li(Co_{1-x}Mg_x)O_2$. This result was confirmed by Raman spectroscopy.

Fig. 8 shows Raman spectra of the (Co/Mg)-coated Ni powers with a different (Co/Mg) mole fraction after immersion in Li/K carbonate at 650 °C for 48 h. The spectrum for $LiCoO_2$ was dominated by strong bands located at 485 and 597 cm$^{-1}$ which from the group factor analysis of the $D_{3h}^5$ spectroscopic symmetry was attributed to the $A_{1g}$ and $E_g$ species, respectively [23]. However, for Co-coated Ni powers, a broad band located around 510 cm$^{-1}$ dominates the spectrum for $LiCo_{1-y}Ni_yO_2$ [12,18]. As the amount of Mg increases, the band of $LiCo_{1-y}Ni_yO_2$ shifted to a higher frequency direction and its intensity decreased drastically due to an increase of the electronic conductivity by Mg diffused into $LiCo_{1-y}Ni_yO_2$ [23,24]. The conductivity of $LiCoO_2$ at room temperature can be increased by over two orders of magnitude by partial substitution of $Co^{3+}$ by $Mg^{2+}$. The conductivity of $LiMg_xCo_{1-x}O_2$ decreased initially and then increased rapidly to achieve a constant value for $x \geq 0.04$ [20].

### 3.3. The (Co/Mg)-coated Ni cathode

The electrode structure is one of the principal factors determining cell performance in MCFCs because the electrode reaction takes place mainly near the meniscus (three phase boundary). For high performance, appropriate pore size distribution (6–10 µm) and porosity (60–80%) is required. The pore size distribution curve of the (Co/Mg)-coated Ni cathode is shown in Fig. 9. The mean pore diameter is about 5–6 µm. The porosity of the (Co/Mg)-coated Ni cathode

coated Ni powder was heated in molten carbonate at 550, 650, 750 and 850 °C. When the (Co/Mg)-coated Ni powder was heated in molten carbonate at 550 °C, the peaks of the $LiCoO_2$ phase were not observed at 45.281°. However, significant $LiCoO_2$ peaks were detected when the powder was heated above 650 °C. Fig. 7 shows XRD patterns of the (Co/Mg)-coated Ni powder with different (Co/Mg) mole fractions after immersion in Li/K carbonate at 650 °C for 48 h. The XRD patterns showed major peaks of $LiCoO_2$ at 18.947, 37.425 and 45.281°. As the Mg content increases, peaks of
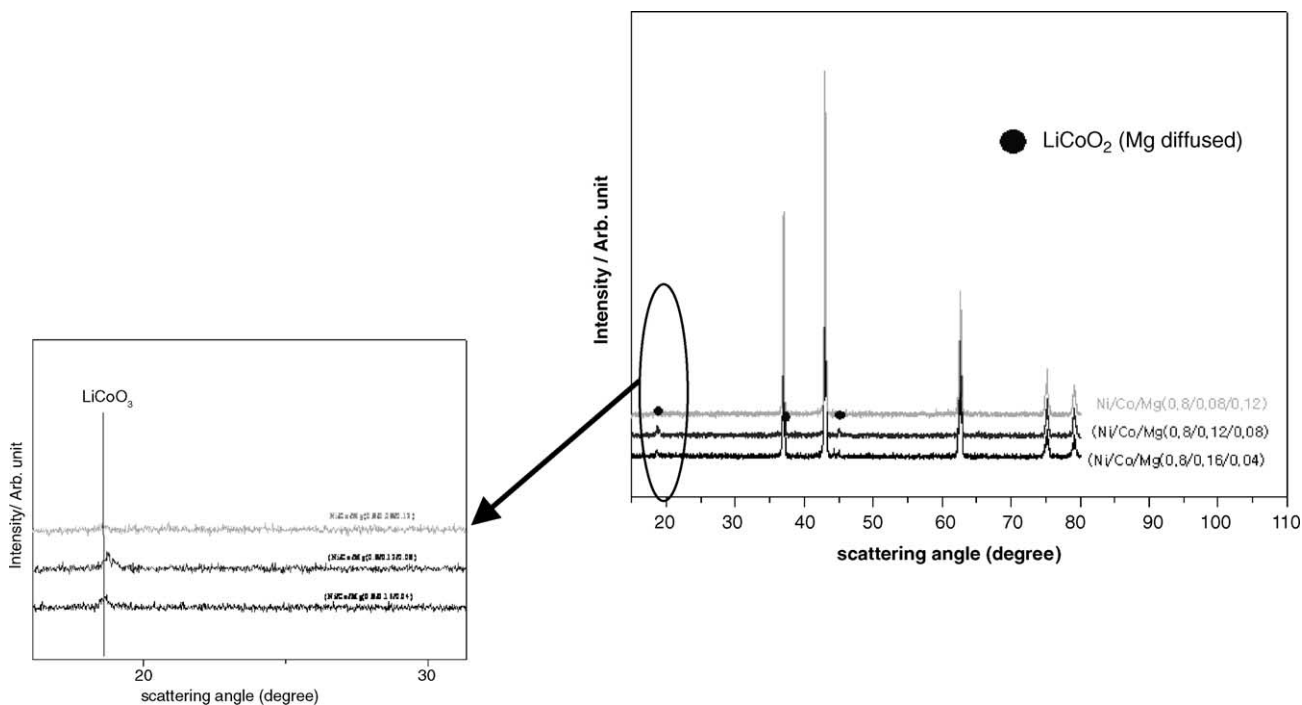


Fig. 7. XRD patterns of (Co/Mg)/Ni with different (Co/Mg) mole fractions after immersion in Li/K carbonate at 650 °C for 48 h.
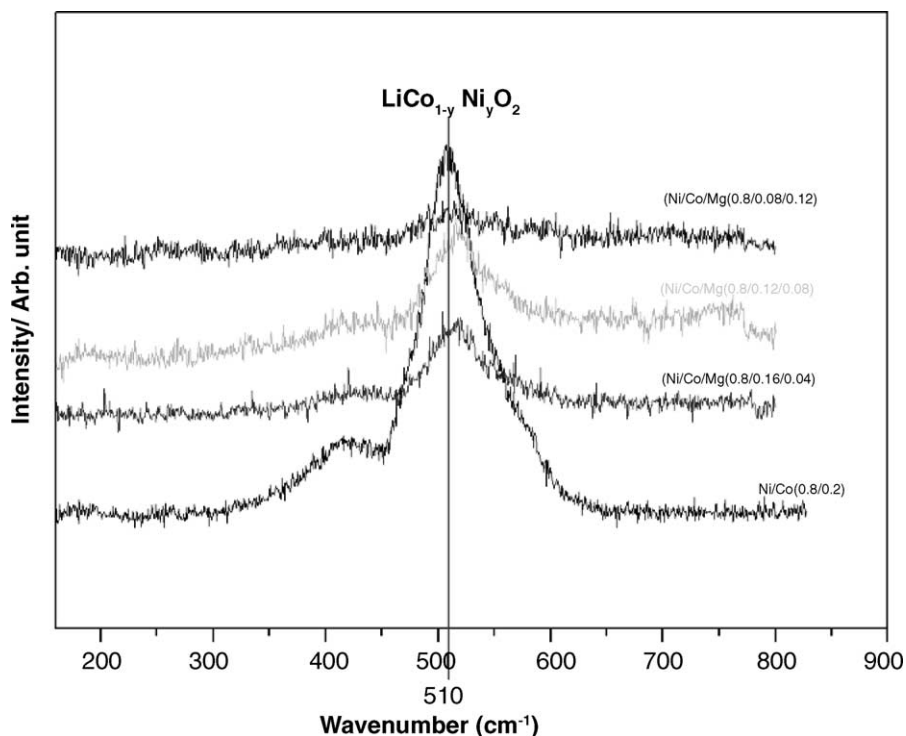
Fig. 8. Raman spectra of (Co/Mg)/Ni with different (Co/Mg) mole fraction after immersion in Li/K carbonate at 650 °C for 48 h.

is about 60–70%, which was measured by a standard test method applying Archimedes' principle (ASTMC378-88). The pore size distribution and the porosity of the (Co/Mg)-coated Ni cathode are almost same as those of the general NiO cathode (pore size: 6–10 µm; porosity: 60–80%). The (Co/Mg)-coated Ni cathode is shown as likely to have a proper pore structure for the MCFC cathode.

Fig. 10 shows SEM images of cross section of the (Co/Mg)-coated Ni cathode after sintering at 1000 °C for 2 h in H$_2$. From SEM images, the morphology of the (Co/Mg)-coated Ni cathode was similar to the pure Ni cathode. It kept the branched structure of primary nickel well and the surface of the NiO was deposited with many small particles, which looks like a homogeneous morphology. The composition of the small particles deposited on the NiO surface was analyzed by line scanning with SEM, which are shown in Fig. 11. Where part (a) is the image of the magnified (Co/Mg)-coated Ni cathode and part (b–e) are the line scanning results of Mg, Co, Ni and O, respectively. From these line-scanning images, we can see that mostly Mg and Co were distributed
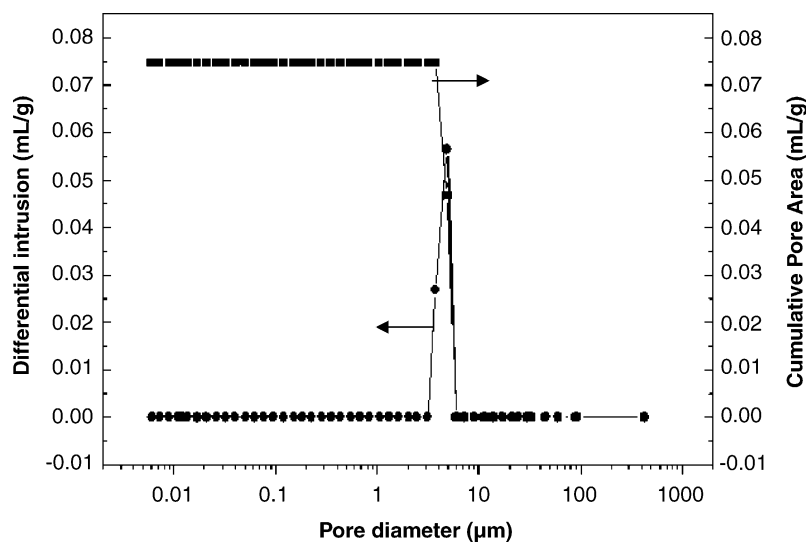


Fig. 9. The pore size distribution curves of the (Co/Mg)-coated Ni cathode.
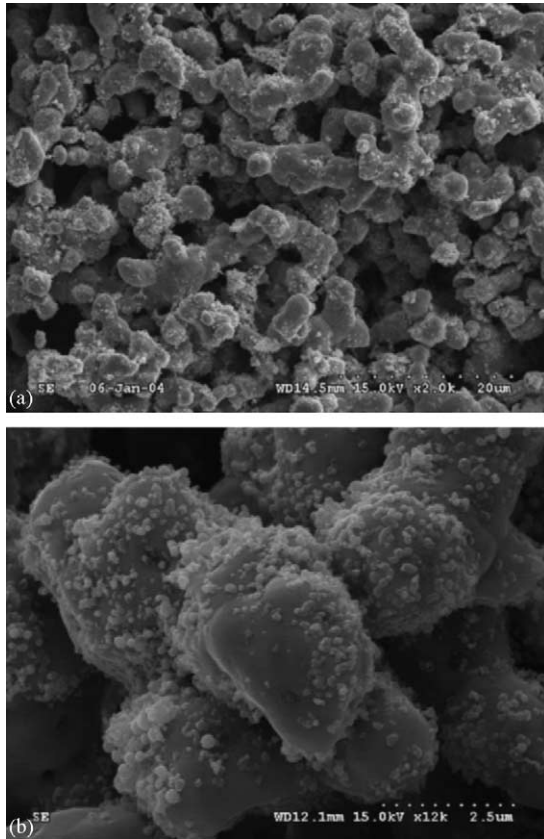
Fig. 10. SEM images of the (Co/Mg)-coated Ni cathode after sintering at 1000 °C for 2 h in $H_2$.

in the small particles. Therefore, we may guess that small particles on the surface of the NiO are the solid solution of $Co_3O_4$/MgO. And furthermore, the results suggest that the (Co/Mg)-coated Ni cathode will form a stable Mg diffused $LiCo_yNi_{2-y}O_2$ phase during cell operation due to in situ lithiation of the (Co/Mg)-coated Ni cathode.

### 3.4. Solubility test

The solubility curves of the NiO cathode, the Co-coated Ni cathode, and the (Co/Mg)-coated Ni cathode in carbonate melt at 650°C under $CO_2$:$O_2$ (67:33) are shown in Fig. 12. The solubility of NiO cathode and Co-coated Ni cathode in carbonate melt were about $3.035 \times 10^{-5}$ and $1.271 \times 10^{-5}$ in mol fractions, respectively [17]. The Co-coated Ni cathode could retard the dissolution of NiO in molten carbonate due to the formation of the stable $LiCo_{1-y}Ni_yO_2$ phase on the surface of NiO [17,19]. However, the solubility of the (Co/Mg)-coated Ni cathode was significantly decreased compared to the other cathodes. It was about $0.661 \times 10^{-5}$ in mole fractions, which was about half of the Co-coated Ni cathode and one-fifth of the NiO cathode. The decrease in solubility of the (Co/Mg)-coated Ni cathode in the carbonate melt was due to the formation of Mg diffused $LiCo_yNi_{1-y}O_2$ on the surface of the NiO, and this phase slows the rate of nickel dissolution in the carbonate melt. The results indicated that $Co_3O_4$/MgO
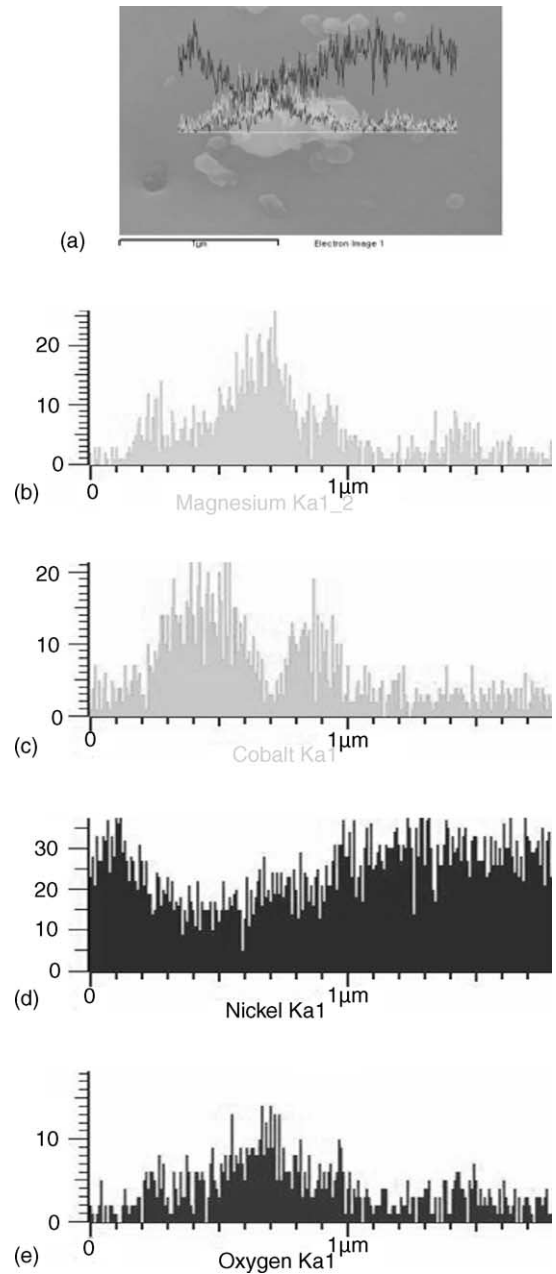


Fig. 11. Line scanning of the (Co/Mg)-coated Ni cathode after sintering at 1000 °C for 2 h in $H_2$.

solid solution deposited NiO cathode might be more stable than the Co-coated NiO cathode in the molten carbonate at 650°C.

Fig. 13 shows the SEM image of the (Co/Mg)-coated Ni cathode before and after the solubility test. The structures of the cathode before and after the solubility test are almost same in the network structure, particle sizes and pore sizes. The results indicate that the prepared (Co/Mg)-coated Ni cathode can be used as a MCFC cathode in longterm operation.
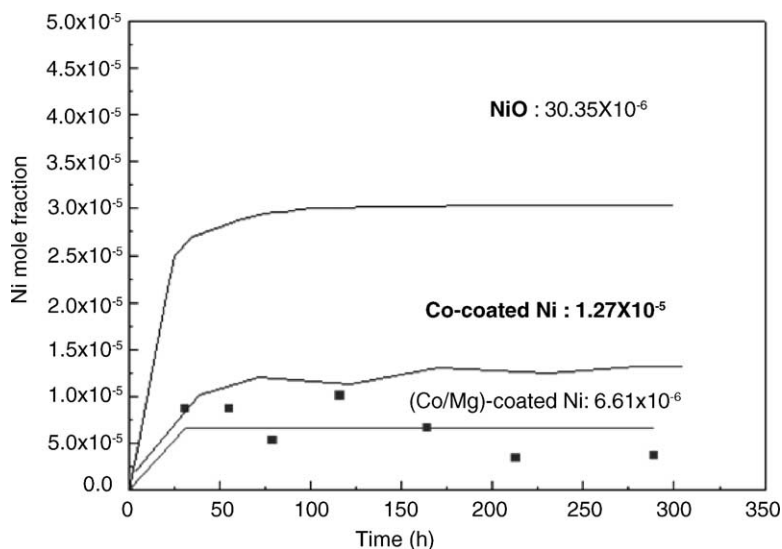
Fig. 12. The solubility of the NiO and the (Co/Mg)-coated Ni cathodes in $(Li_{0.62}K_{0.38})_2CO_3$ at 650 °C under $CO_2$:$O_2$ (67:33).


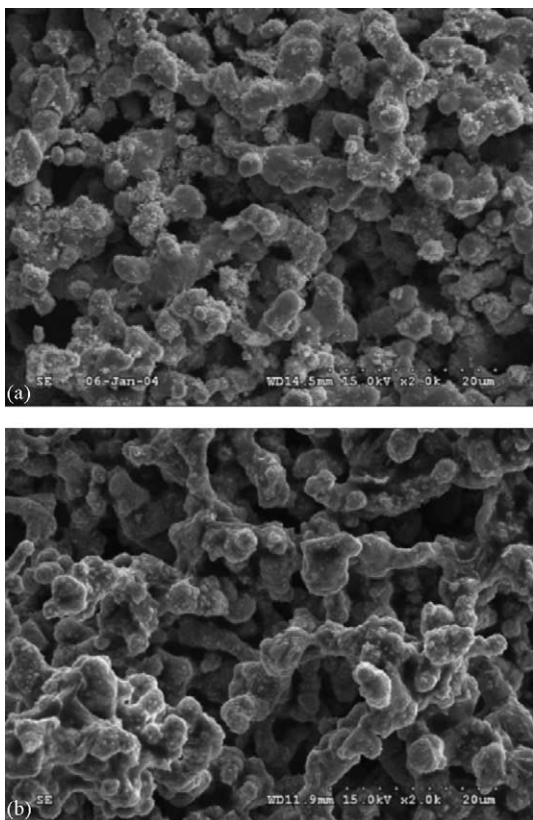
Fig. 13. SEM images of the (Co/Mg)-coated Ni cathode (a) before and (b) after solubility test at 650 °C in $CO_2$:$O_2$ (67:33).

## 4. Conclusion

A new cathode material for a MCFC have been prepared by a coating of Co/Mg solid solution on the Ni powder surface using a PVA assisted sol–gel method. The average pore size of the (Co/Mg)-coated Ni cathodes are almost same as the NiO cathode.

The solubility of the (Co/Mg)-coated Ni cathode is about half that of the Co-coated Ni cathode and one-fifth of the NiO cathode. The decrease in solubility of the (Co/Mg)-coated Ni cathode in a carbonate melt is due to the formation of Mg diffused $LiCo_yNi_{1-y}O_2$ on the surface of the NiO and this phase slows the rate of nickel dissolution in $(Li_{0.62}K_{0.38})CO_3$ under $CO_2$:$O_2$ (67:33%) atmosphere.

Further studies are in progress in order to investigate the electrochemical performance of the (Co/Mg)-coated Ni cathode.

## Acknowledgement

## References

[1] G.L. Lee, J.R. Selman, L. Pomp, J. Electrochem. Soc. 140 (2) (1993) 390.
[2] N.Q. Minh, J. Power Sources 24 (1998) 1.
[3] Molten carbonate fuel cell technology, in: J.R. Selman, D.A. Shores, H.C. Maru, I. Uchida (Eds.), PV90-16, The Electrochemical Society Softbound Proceeding Series, Pennington, NJ, 1990.
[4] K. Ota, S. Mitsushima, S. Kato, S. Asano, H. Yoshitake, N. Kamiya, J. Electrochem. Soc. 139 (1992) 667.
[5] Y. Ito, K. Tsuru, J. Oishi, Y. Miyazaki, K. Teruo, J. Power Sources 23 (4) (1998) 357–364.
[6] P. Ganesan, H. Colon, B. Haran, R. White, B.N. PoPov, J. Power Sources 111 (2002) 109–120.
[7] S. Terada, K. Higaki, I. Nagashima, Y. Ito, J. Power Sources 83 (1999) 178.
[8] L. Plomp, E.F. Sitters, C. Vessies, F.C. Eckes, J. Electrochem. Soc. 138 (1991) 629.

[9] C. Lagergren, A. Lundblad, B. Bergman, J. Electrochem. Soc. 141 (1994) 2959.

[10] L. Giogi, M. Carewska, S. Scaccia, E. Simonetti, F. Zarzana, Denki Kagaku 64 (1996) 482.

[11] T. Fukui, S. Ohara, H. Okawa, T. Hotta, M. Naito, J. Power Sources 86 (2000) 340.

[12] S. Kuk, Y. Seck Song, K. Kim, J. Power Sources 83 (1999) 50.

[13] L. Plomp, J.B.J. Veldhuis, E.F. Sitters, S.B. van der Molen, J. Power Sources 39 (1992) 369.

[14] L. Giorgi, M. Carewska, M. Patriarca, S. Scaccia, E. Simonetti, A. Di Bartolomeo, J. Power Sources 49 (1994) 227.

[15] A. Lundblad, S. Schwartz, B. Bergman, J. Power Sources 90 (2000) 224.

[16] T.M.T.N. Tennakoon, G. Lindbergh, B. Bergman, J. Electrochem. Soc. 144 (1997) 2296.

[17] H. Lee, M. Hong, S. Bae, H. Lee, E. Park, K. Kim, J. Mater. Chem. 13 (10) (2003) 2626–2632.

[18] S.T. Kuk, Y.S. Song, S.I. Suh, K. Kim, J. Mater. Chem. 11 (2001) 630–635.

[19] M.Z. Hong, S.C. Bae, H.S. Lee, H.C. Lee, Y.M. Kim, K. Kim, Electrochim. Acta 48 (28) (2003) 4213–4221.

[20] H. Tukamoto, A.R. West, J. Electrochem. Soc. 144 (9) (1997) 3164.

[21] J.P. Cho, Chem. Mater. 12 (2000) 3089–3094.

[22] E.M. Levin, et al., Phase Diagrams for Ceramists, The American Ceramic Society, 1964, p. 52.

[23] M. Inaba, Y. Todzuka, H. Yoshida, Y. Grincourt, A. Tasaka, Chem. Lett. (1995) 889.

[24] C. Jilien, M.A. Camacho-Lopez, T. Mohan, S. Chitra, P. Kalyani, S. Gopukumar, Solid State Ionics 135 (2000) 241.